LA-UR- 09-08187

Approved for public release;
distribution is unlimited.

Title:	Numerical Modeling of Two-Phase Behavior in the PEFC Gas Diffusion Layer
Author(s):	Partha P. Mukherjee, Qinjun Kang, Rangachary Mukundan, and Rodney L. Borup
Submitted to:	ECS Transactions for the 2009 Fuel Cell Seminar

Form 836 (8/00)

Numerical Modeling of Two-Phase Behavior in the PEFC Gas Diffusion Layer

P. P. Mukherjee, Q. Kang, R. Mukundan, and R. L. Borup

Los Alamos National Laboratory, Los Alamos, New Mexico 87545, USA

A critical performance limitation in the polymer electrolyte fuel cell (PEFC) is attributed to the mass transport loss originating from suboptimal liquid water transport and flooding phenomena. Liquid water can block the porous pathways in the fibrous gas diffusion layer (GDL) and the catalyst layer (CL), thus hindering oxygen transport from the flow field to the electrochemically actives sites in the catalyst layer. The cathode GDL is the component primarily responsible for facilitating gas and liquid transport, therefore plays a major role in determining the water management of a PEFC and hence the mass transport loss. The underlying pore morphology and wetting characteristics have significant influence on the flooding dynamics in the GDL. In this paper, the study of the two-phase behavior and the durability implications due to the wetting characteristics in the carbon paper GDL are presented using a pore-scale modeling framework.

Introduction

The gas diffusion layer plays a critical role in the overall PEFC performance, especially in the mass transport control regime characterized by high current density operation (1, 2). Liquid water blocks the porous pathways in the catalyst layer and gas diffusion layer thereby causing hindered oxygen transport from the channel to the active reaction sites in the CL. This phenomenon is known as "flooding" and is perceived as the primary mechanism leading to the limiting current behavior in the cell performance. The pore morphology and wetting characteristics of the cathode GDL are of paramount importance in the effective PEFC water management (1,2) aimed at maintaining a delicate balance between reactant transport from the gas channels and water removal from the electrochemically active sites. The multi-faceted functionality of a GDL includes reactant distribution, liquid water transport, electron transport, heat conduction and mechanical support to the membrane-electrode-assembly. Carbon-fiber based porous materials, namely non-woven carbon paper and woven carbon cloth, with thickness ~200-300 μm, have received wide acceptance as materials of choice for the PEFC GDL owing to high porosity (~ 70% or higher) and good electrical/thermal conductivity. Mathias *et al.* (3) provided a comprehensive overview of the GDL structure and functions. The beginning-of-life (fresh) GDL exhibits fully hydrophobic characteristics, which facilities liquid water transport and hence reduces flooding. Experimental data, however, suggest that the GDL loses hydrophobicity over prolonged PEFC operation and becomes prone to enhanced flooding. Borup and co-workers (2,4) have reported the GDL durability issues due to the loss of hydrophobicity from their extensive experimental investigation. Figure 1 summarizes the change in contact angles of different types of carbon paper GDL with ageing (1).

In the last few years, water management research has received wide attention, evidenced by the development of several macroscopic models for liquid water transport in PEFCs (5-9). The macroscopic models for liquid water transport, reported in the

literature, are based on the theory of volume averaging and treat the GDL as a macrohomogeneous porous layer. Due to the macroscopic nature, the current models fail to resolve the influence of the pore morphology and wetting characteristics of the GDL on the underlying two-phase dynamics. Although substantial research, both modeling and experimental, has been conducted to study flooding and water transport in PEFCs, there is a lack of fundamental understanding of the structure-wettability influence on the underlying two-phase behavior, which affects the cell performance. In this work, a pore-scale modeling framework is presented to study the structure-wettability-durability interplay in the context of flooding behavior in the non-woven carbon paper GDL of a PEFC.

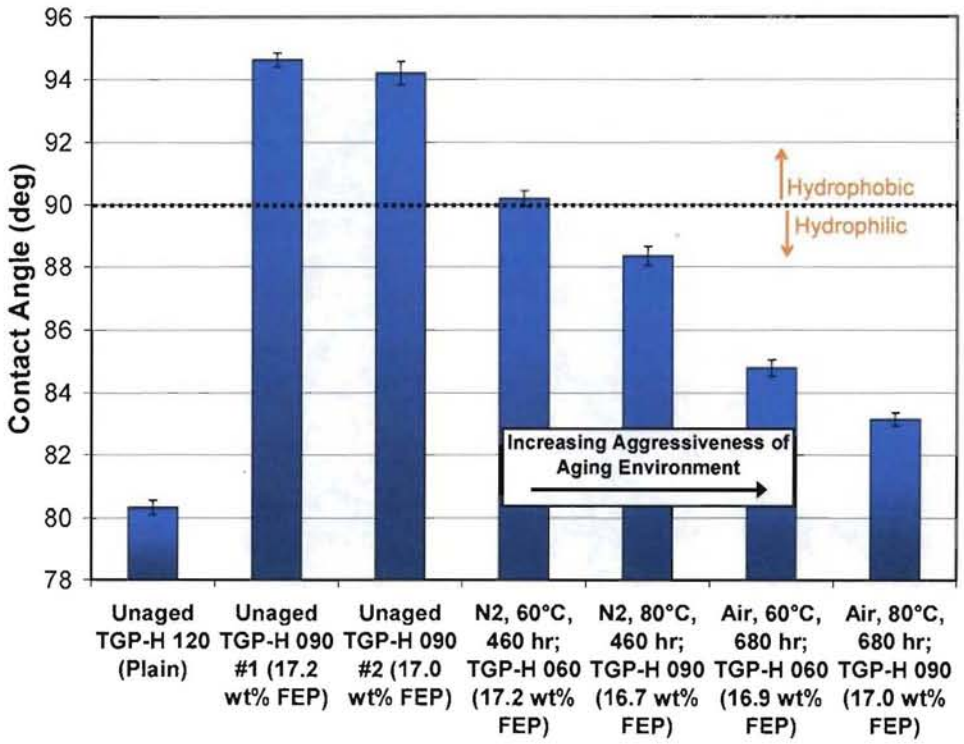

Figure 1: Loss of hydrophobicity of different types of GDL with ageing (2).

Modeling Approach

The pore-scale modeling framework consists of: (1) fibrous microstructure reconstruction, and (2) two-phase lattice Boltzmann (LB) model for two-phase transport in the GDL microstructure.

Microstructure Generation

Detailed description of a porous microstructure is an essential prerequisite to pore-scale modeling. The 3-D volume data of a porous sample can be obtained either by experimental imaging or by stochastic simulation method. Recent ongoing efforts at Los Alamos National Laboratory (LANL) in generating 3-D GDL microstrcutures using experimental imaging include both invasive and non-invasive methods. Garzon and co-workers (10) have recently demonstrated the generation of 3-D GDL microstructures using the non-invasive X-Ray microtomography technique. Figure 2(a) shows representative X-Ray microtomography images of non-woven GDL microstructures with and without the microporous layer (MPL). Concurrent to the X-Ray tomography method,

we are proposing here for the first time the 3-D reconstruction of non-woven GDL microstructures using digital volume imaging (DVI), which is a block-face fluorescence imaging technique (11,12). In this technique, the porous sample, embedded in a polymeric resin, is repeatedly sectioned and imaged (11,12) These 2-D cross-sectional images are then combined to reconstruct the 3-D microstructure. The DVI technique is a destructive imaging method as opposed to the non-invasive X-Ray microtomography imaging. Figure 2(b) shows a representative polyester non-woven fibrous structure generated using the DVI technique by Pourdeyhimi and co-workers (12), which demonstrates the prospect of the DVI method in the reconstruction of 3-D non-woven GDL mcirostructures. The 3-D reconstruction of GDL microstructure using the DVI method is currently underway and will be reported in a future communication.

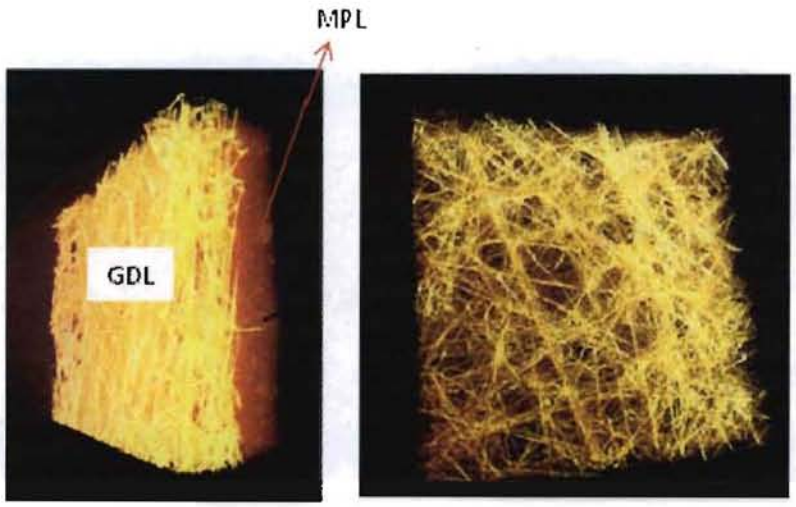

(a) PEFC GDL Microstructure using X-Ray Microtomography (10)

(b) Polyester Fabric using DVI (12)

Figure 2: Representative 3-D non-woven fibrous microstructures generated using experimental imaging.

The stochastic simulation technique, on the other hand, creates 3-D realization of the non-woven carbon paper GDL based on structural inputs, namely fiber diameter, fiber orientation and porosity which can be obtained either directly from the fabrication specifications or indirectly from the SEM (scanning electron microscope) micrographs or

by experimental techniques. Details about the carbon paper GDL microstructure reconstruction method along with the underlying assumptions are elaborated in our recent work (13). Briefly, the stochastic reconstruction technique is a Poisson line process with one-parametric directional distribution where the fibers are realized as circular cylinders with a given diameter and the directional distribution provieds in-plane/through-plane anisotropy in the reconstructed GDL microstructure (13). Figure 3 shows the reconstructed microstructure of a typical non-woven, carbon paper GDL with porosity around 72% and thickness of 180 μm along with the estimated pore size distribution (12).

In this work, a 3-D reconstructed carbon paper GDL microstructure using the stochastic simulation method is deployed in the subsequent tw-phase pore-scale simulations.

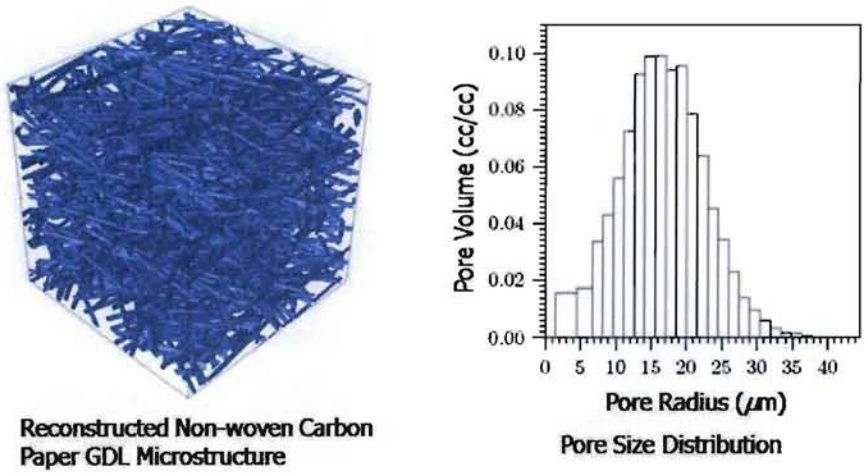

Figure 3: Reconstructed non-woven carbon paper GDL microstructure along with the estimated pore size distribution.

Two-Phase Lattice Boltzmann Model

In recent years, the lattice Boltzmann (LB) method, owing to its excellent numerical stability and constitutive versatility, has developed into a powerful technique for simulating fluid flows and is particularly successful in fluid flow applications involving interfacial dynamics and complex geometries (14). The LB method is a particle based numerical approach, which considers a flow being composed of a collection of pseudo-particles residing on the nodes of an underlying lattice structure which interact according to a velocity distribution function. It is a scale-bridging numerical scheme which incorporates simplified kinetic models to capture microscopic or mesoscopic flow physics and yet the macroscopic averaged quantities satisfy the desired macroscopic equations (14).

The two-phase lattice Boltzmann model developed in this work is based on the interaction potential model, originally proposed by Shan and Chen (15). This model introduces k distribution functions for a fluid mixture comprising of k components. Each distribution function represents a fluid component and satisfies the evolution equation. The interaction between particles at neighboring lattice sites is included in the kinetics through a set of potentials. The LB equation for the kth component can be written as:

$$f_i^k(\mathbf{x}+\mathbf{e}_i\delta_t, t+\delta_t) - f_i^k(\mathbf{x},t) = -\frac{f_i^k(\mathbf{x},t) - f_i^{k(eq)}(\mathbf{x},t)}{\tau_k} \qquad [1]$$

where $f_i^k(\mathbf{x},t)$ is the number density distribution function for the kth component in the ith velocity direction at position $\mathbf{x}$ and time t, and δ_t is the time increment. In the term on the right-hand side, τ_k is the relaxation time of the kth component in lattice unit, and $f_i^{k(eq)}(\mathbf{x},t)$ is the corresponding equilibrium distribution function. The right-hand-side of Eq. [1] represents the collision term, which is simplified to the equilibrium distribution function $f_i^{k(eq)}(\mathbf{x},t)$ by the so-called BGK (Bhatnagar-Gross-Krook), or the single-time relaxation approximation (16). A three-dimensional 19-speed lattice (D3Q19, where D is the dimension and Q is the number of velocity directions), shown schematically along with the velocity directions in Fig. 4, is used. Surface tension between the two phases is realized through a fluid/fluid interaction force and the wall adhesion effect i.e. the contact angle is incorporated via a fluid/solid interaction force. The details of the two-phase lattice Boltzmann model developed for this study are furnished in Refs. (15,17,18-20).

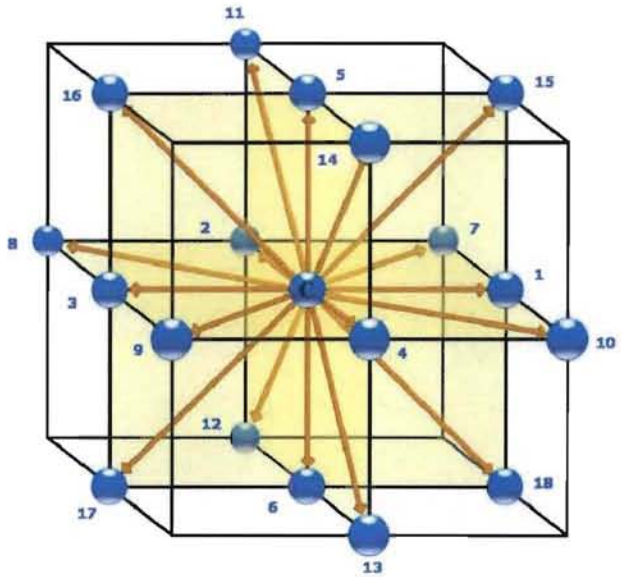

Figure 4: D3Q19 lattice structure.

Two-Phase Numerical Experiment and Setup

In this study, a numerical experiment is specifically designed to simulate a *quasi-static displacement experiment*, detailed elsewhere in the literature in the context of geologic porous media transport (21), for simulating immiscible, two-phase transport in the reconstructed GDL microstructure. It is important to note that the two-phase transport in the PEFC GDL is characterized by capillary transport as evidenced by very low Capillary number ($Ca = \mu_2 U_2 / \sigma \sim 10^{-6}$) operation (18-20). In the Capillary number expression, U_2 and μ_2 are the non-wetting phase Darcy velocity and dynamic viscosity respectively, σ is the surface tension. In the capillary transport regime, surface forces dominate over the inertial, viscous and gravity forces (18-20).

In the numerical setup, a non-wetting phase (NWP) reservoir is added to the GDL microstructure at the front end and a wetting phase (WP) reservoir is added at the back end (17). For the drainage simulation in the GDL, liquid water (NWP) is injected into the air (WP) saturated domain, thereby mimicking the quasi-static displacement experiment in an *ex situ* setup. The drainage process is simulated starting with zero capillary pressure, by fixing the NWP and WP reservoir pressures to be equal. Then the capillary pressure is increased incrementally by decreasing the WP reservoir pressure while maintaining the

NWP reservoir pressure at the fixed initial value. The details of the numerical setup corresponding to the drainage simulation are furnished in Refs. (18,20). For the subsequent two-phase simulations, a reconstructed GDL structure with 100×100×100 lattice points is used keeping in mind the significant computational overhead in LB calculations. The primary objective of the quasi-static displacement simulation is to study the liquid water behavior through the fibrous GDL structure and the influence owing to the pore-morphology and wetting characteristics.

Results and Discussion

Figure 5 shows the liquid water distribution as well as the invasion pattern from the *displacement simulation* with increasing capillary pressure in the initially air-saturated carbon paper GDL characterized by hydrophobic wetting characteristics with a static contact angle of 140^0. The fully hydrophobic GDL represents a beginning-of-life sample. At the initially very low capillary pressure, the invading front overcomes the barrier pressure only at some preferential locations depending upon the pore size along with the emergence of droplets owing to strong hydrophobicity. As the capillary pressure increases, several liquid water fronts start to penetrate into the air occupied domain. Further increase in capillary pressure exhibits growth of droplets at two invasion fronts, followed by the coalescence of the drops and collapsing into a single front. This newly formed front then invades into the less tortuous in-plane direction. Additionally, emergence of tiny droplets and subsequent growth can be observed in the constricted pores in the vicinity of the inlet region primarily due to strong wall adhesion forces from interactions with highly hydrophobic fibers with the increasing capillary pressure. One of the several invading fronts finally reaches the air reservoir, physically the GDL/channel interface, at a preferential location corresponding to the capillary pressure and is also referred to as the bubble point. Additionally, 2-D liquid water saturation maps on different cross-sections along the GDL through-plane direction corresponding to the liquid water saturation level at the bubble point are shown in Fig. 6 which demonstrates the porous pathways actually available for oxygen transport from the channel to the CL reaction sites.

Figure 7 shows the invasion pattern of liquid water from the *displacement simulation* with increasing capillary pressure in the initially air-saturated carbon paper GDL microstructure characterized by *mixed wettability*. As mentioned earlier, after prolonged operation in a PEFC, the carbon fibers tend to lose hydrophobicity and the GDL structure exhibits hydrophobic and hydrophilic pores (2). In this simulation, 50% of the pore volume is rendered hydrophilic, which are assumed to be randomly dispersed throughout the GDL structure, thereby characterizing an aged GDL. The hydrophobic pores are characterized with a static contact angle of 140^0 and the hydrophilic pores with 80^0. At the initially very low capillary pressure, the invading liquid water exhibits both droplet formation in the hydrophobic pores and film formation due to the hydrophilic pores. With increasing capillary pressure, liquid water films tend to merge and assists in front movement. The front propagation is dominated by the film formation and subsequent merging phenomena. The underlying anisotropy in the GDL microstructure fails to assist in the branching and in-plane movement as in the case of a purely hydrophobic GDL. Toward the bubble point, the aged GDL displays liquid water slug formation, instead of fingers and evidently leads to higher saturation level and enhanced flooding. Figure 8 shows the 2-D liquid water saturation maps on different cross-sections along the GDL through-plane direction corresponding to the liquid water distribution at the bubble point.

These 2-D saturation maps clearly demonstrate the effect of hydrophilic pores on the enhanced occupancy of the porous pathways and hence the elevated resistance to oxygen transport from the channel to the CL reaction sites.

Finally, it is worth mentioning that the LB simulation is indeed able to capture the influence of the pore wetting characteristics on the intricate liquid water dynamics including droplet interaction, film formation and flooding front propagation through the GDL microstructure.

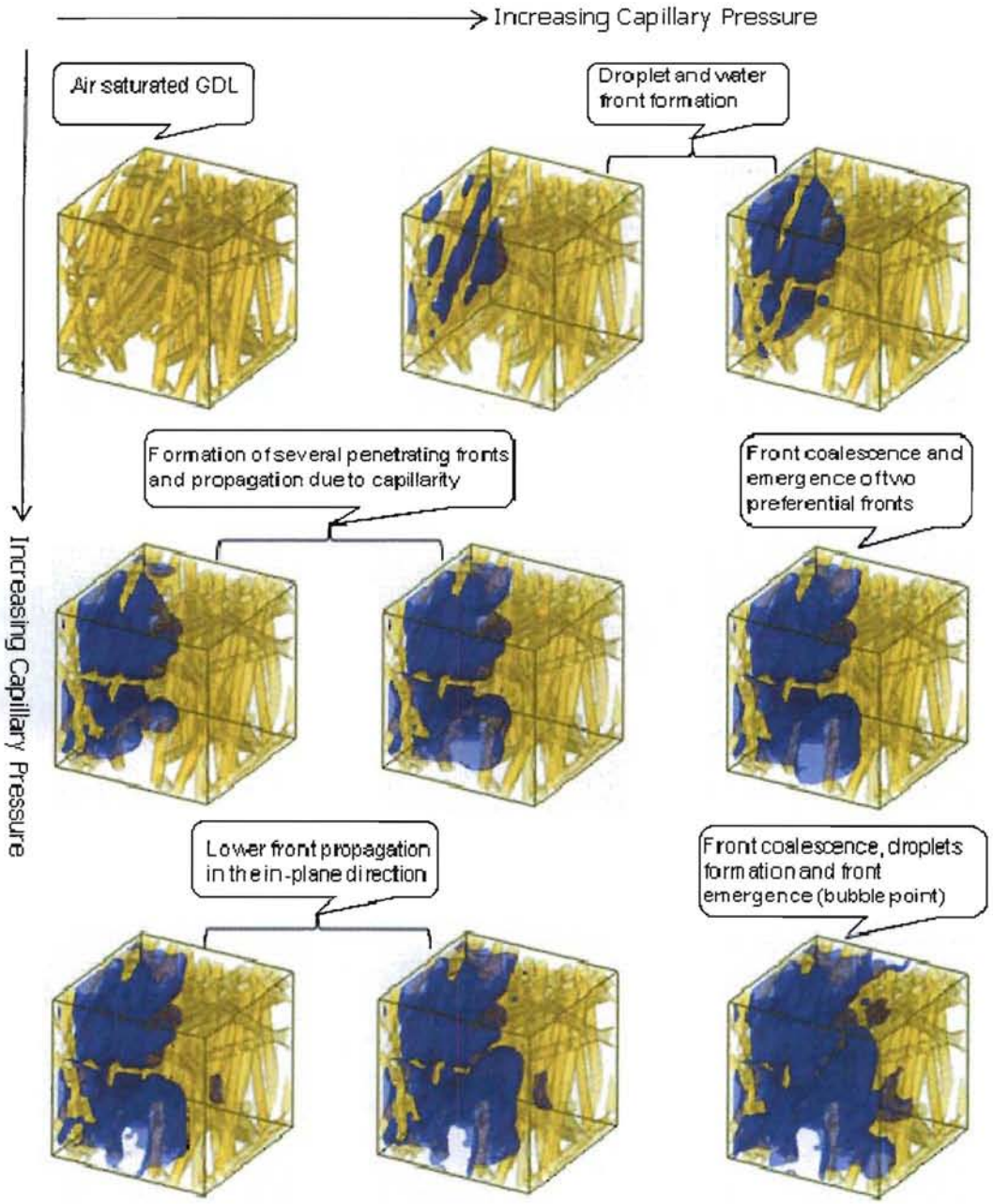

Figure 5: Advancing liquid water front with increasing capillary pressure through the fully hydrophobic GDL microstructure from the displacement simulation.

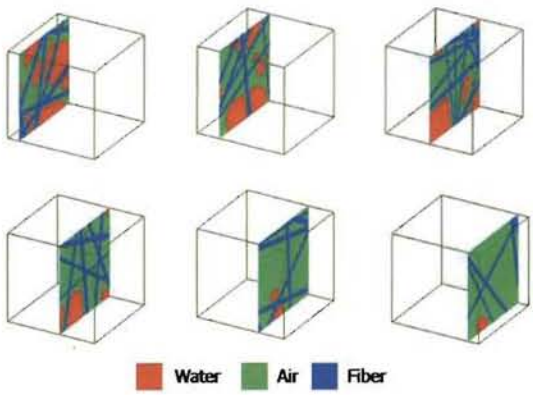

Figure 6: 2-D phase distribution maps on several cross-sections along the through-plane direction in the fully hydrophobic GDL structure from the displacement simulation.

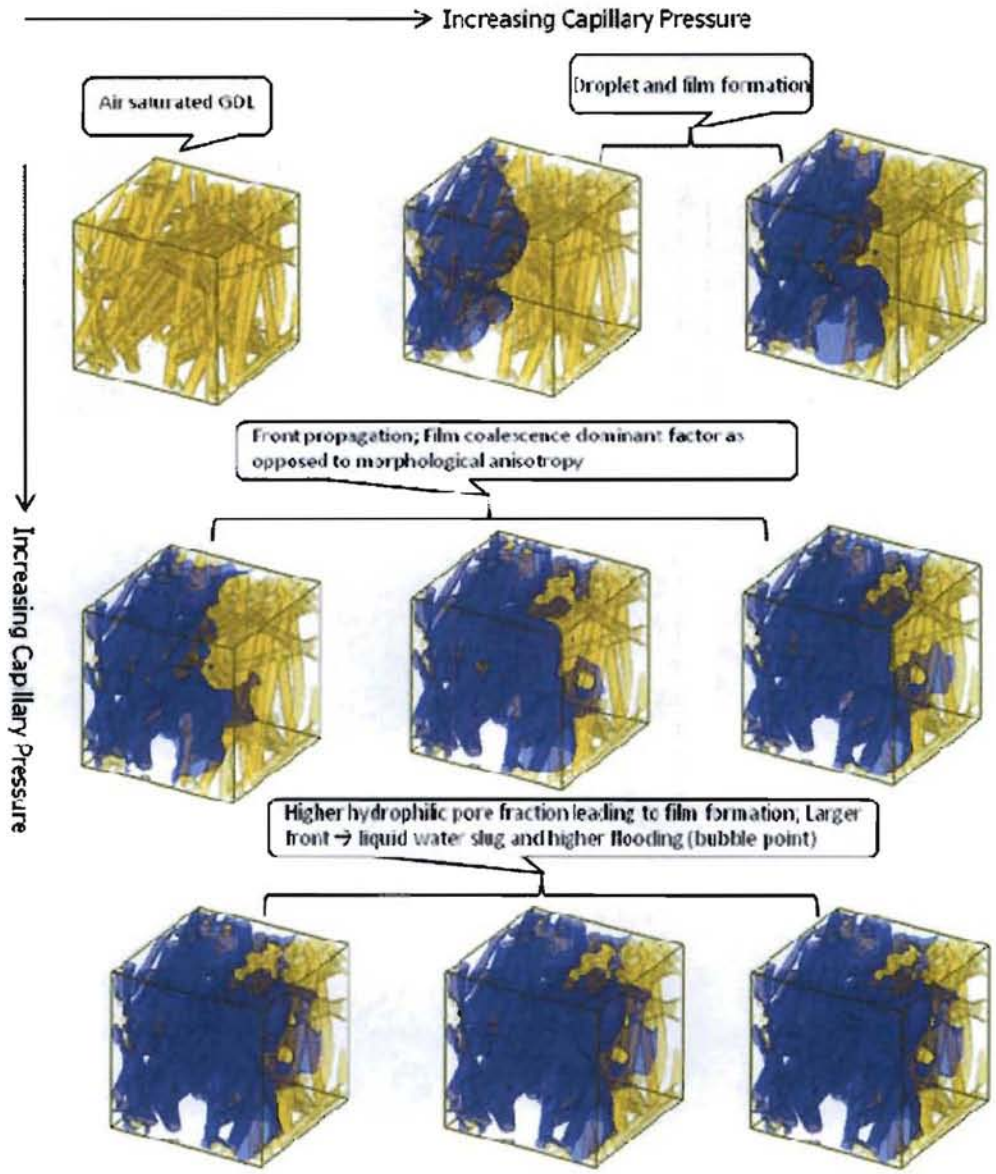

Figure 7: Advancing liquid water front with increasing capillary pressure through the mixed wet GDL microstructure with 50% hydrophilic pores from the displacement simulation.

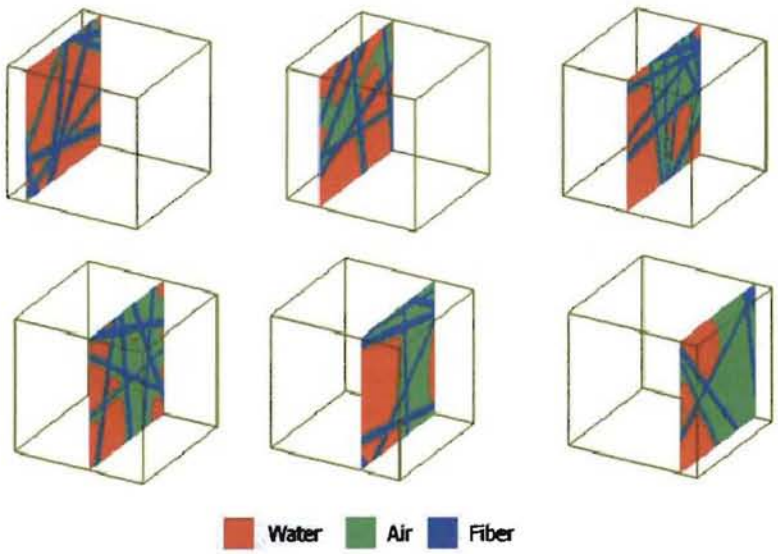

Figure 8: 2-D phase distribution maps on several cross-sections along the through-plane direction in the mixed wet GDL microstructure with 50% hydrophilic pores from the displacement simulation.

Conclusions

The gas diffusion layer plays a crucial role in the overall PEFC performance due to the transport limitation in the presence of liquid water and flooding phenomena. The loss of hydrophobicity owing to ageing further affects the flooding behavior and hence the cell performance. In this work, the development of a pore-scale modeling formalism consisting of microstructure reconstruction and a two-phase lattice Boltzmann model is presented in order to reveal the wettability influence on the flooding dynamics in the PEFC GDL. The liquid water transport in a fresh non-woven GDL structure with purely hydrophobic wetting characteristics shows intricate interfacial dynamics including droplet interactions, flooding front formation, in-plane movement and front merging. The mixed wet structure, representative of an aged GDL, exhibits film formation and merging as the primary mechanism of liquid water front movement, which ultimately results in enhanced flooding. Additionally, the DVI technique is proposed to experimentally image realistic non-woven GDL microstructures, which will be used as input into two-phase pore-scale modeling.

Acknowledgments

PPM would like to thank V. P. Schulz, J. Becker and A. Wiegmann from Fraunhofer ITWM, Germany, for collaboration with GDL stochastic microstructure reconstruction. Financial support from Los Alamos National Laboratory LDRD program and DOE EERE Fuel Cell Technologies Program (Program Manager: Nancy Garland) is gratefully acknowledged.

References

1. C. Y. Wang, *Chem. Rev.*, (*Washington, DC*), **104**, 4727 (2004).
2. D. L. Wood III and R. L. Borup, in *Polymer Electrolyte Fuel Cell Durability*, F. N. Buchi, M. Inaba, and T. J. Schmidt, Editors, Springer, New York, 159 (2009).

3. M. F. Mathias, J. Roth, J. Fleming, and W. Lehnert, in *Handbook of Fuel Cells – Fundamentals, Technology and Applications*, W. Lietsich, A. Lamm and H. A. Gasteiger, Editors, Ch. 42, John Wiley & Sons, Chicester, **3**, 517 (2003).
4. R. L. Borup *et al.*, *Chemical Reviews*, **107**, 3904 (2007).
5. U. Pasaogullari and C. Y. Wang, *J. Electrochem. Soc.*, **151**, 399 (2004).
6. Y. Wang and C. Y. Wang, *J. Electrochem. Soc.*, **153**, A1193 (2006).
7. A. Z. Weber and J. Newman, *J. Electrochem. Soc.*, **152**, A677 (2005).
8. J. Nam and M. Kaviany, *Int. J. Heat Mass Transfer*, **46**, 4595 (2003).
9. W. He, J. S. Yi, and T. V. Nguyen, *AIChE J.*, **46**, 2053 (2000).
10. M. Nelson, F. Garzon *et al.*, Presentation at the 215th ECS Meeting, San Francisco, CA, USA, May 24-29 (2009).
11. D. Chinn, P. Ostendorp, M. Haugh, R. Kershmann, T. Kurfess, A. Claudet, T. Tucker, *J. Manuf. Sci. Eng.*, **126**, 813 (2004).
12. S. Jaganathan, H. V. Tafreshi, B. Pourdeyhimi, *J. Colloid Interface Sci.*, **326**, 166 (2008).
13. V. P. Schulz, J. Becker, A. Wiegmann, P. P. Mukherjee, and C. Y. Wang, *J. Electrochem. Soc.*, **154**, B419 (2007).
14. S. Chen and G. D. Doolen, *Ann. Rev. Fluid Mech.*, **30**, 329 (1998).
15. X. Shan and H. Chen, *Phys. Rev. E*, **47**, 1815, 1993.
16. P. Bhatnagar, E. Gross, and M. Krook, *Phys. Rev.*, **94,** 511 (1954).
17. Q. Kang, D. Zhang, and S. Chen, *J. Fluid Mech.*, **545**, 41 (2005).
18. P. P. Mukherjee, *PhD Dissertation*, Pennsylvania State University, University Park, PA, USA (2007).
19. P. P. Mukherjee, P. K. Sinha, and C. Y. Wang, *J. Mater. Chem.*, **17**, 3089 (2007).
20. P. P. Mukherjee, C. Y. Wang, and Q. Kang, *Electrochim. Acta*, **54**, 6861 (2009).
21. J. Bear, *Dynamics of Fluids in Porous Media*, Dover, New York (1972).